Landscape of the PARKIN-dependent ubiquitylome in response to mitochondrial depolarization

Shireen A. Sarraf, **Malavika Raman**, **Virginia Guarani-Pereira**, **Mathew E. Sowa**, **Edward L. Huttlin**, **Steven P. Gygi**, and **J. Wade Harper**[*]

Department of Cell Biology, Harvard Medical School, 240 Longwood Ave, Boston MA 02115

Abstract

The PARKIN (PARK2) ubiquitin ligase and its regulatory kinase PINK1 (PARK6), often mutated in familial early onset Parkinson's Disease (PD), play central roles in mitochondrial homeostasis and mitophagy.[1–3] While PARKIN is recruited to the mitochondrial outer membrane (MOM) upon depolarization via PINK1 action and can ubiquitylate Porin, Mitofusin, and Miro proteins on the MOM,[1,4–11] the full repertoire of PARKIN substrates – the PARKIN-dependent ubiquitylome - remains poorly defined. Here we employ quantitative diGLY capture proteomics[12,13] to elucidate the ubiquitylation site-specificity and topology of PARKIN-dependent target modification in response to mitochondrial depolarization. Hundreds of dynamically regulated ubiquitylation sites in dozens of proteins were identified, with strong enrichment for MOM proteins, indicating that PARKIN dramatically alters the ubiquitylation status of the mitochondrial proteome. Using complementary interaction proteomics, we found depolarization-dependent PARKIN association with numerous MOM targets, autophagy receptors, and the proteasome. Mutation of PARKIN's active site residue C431, which has been found mutated in PD patients, largely disrupts these associations. Structural and topological analysis revealed extensive conservation of PARKIN-dependent ubiquitylation sites on cytoplasmic domains in vertebrate and *D. melanogaster* MOM proteins. These studies provide a resource for understanding how the PINK1-PARKIN pathway re-sculpts the proteome to support mitochondrial homeostasis.

PARKIN, a RING-HECT hybrid E3 ubiquitin ligase,[14] is recruited to the MOM in cancer cell lines, mouse embryo fibroblasts (MEFs), and primary neurons to promote mitophagy in response to mitochondrial depolarization.[1,2,15,16] This process requires PINK1, which binds the MOM translocase (TOMM) complex and phosphorylates PARKIN on multiple residues to promote MOM localization and ligase activation.[17–20] The best understood PARKIN

---

[*]Send correspondence to: wade_harper@hms.harvard.edu.

substrates are MFN1/2 and RHOT1/2 (MIRO in *Drosophila*), MOM-tethered GTPases whose PARKIN-dependent proteasome turnover alters fission-fusion cycles and microtubule-dependent trafficking of mitochondria, respectively.[1,5,6,7,8,10,11] The MOM porin proteins VDAC1/2/3 are also ubiquitylated by PARKIN, and are required for PARKIN localization on mitochondria through a poorly understood mechanism.[9,21] Proteomic studies of purified mitochondria have also identified additional proteins whose abundance is either decreased or increased upon PARKIN activation or mitochondrial depolarization,[1,4] but precisely how these proteins are regulated and the extent to which ubiquitin is involved is unclear. Consequently, we do not have a comprehensive understanding of cellular PARKIN targets, which is critical for elucidating how PARKIN promotes mitochondrial homeostasis. Moreover, for the vast majority of E3s, including PARKIN, the extent to which ubiquitin transfer is site-specific and signal-dependent is largely unknown, and a global understanding of site-specificity across a wide range of substrates is lacking for any E3. Such information is necessary for decoding the cellular and molecular topology of E3 function and for defining how the ubiquitin system re-sculpts the proteome.

We set out to systematically identify cellular PARKIN-dependent ubiquitylation targets and the dynamics of modification in a site-specific manner using quantitative diGLY (QdiGLY) proteomics. QdiGLY merges antibody-based capture of "diGLY remnant" containing peptides (marking ubiquitylated proteins after trypsinolysis) and stable isotopic labeling with amino acids in culture (SILAC) to identify ubiquitylation sites that are dynamically induced, in this case, upon mitochondrial depolarization.[12,13] To overcome inherent stochastic sampling for low abundance diGLY peptides (see Figure S1a,b),[12,13] we performed 73 control and QdiGLY profiling experiments in 4 cell lines with and without elevated PARKIN levels (~10-fold) (Figure S2a) in a 3-tiered manner, varying the length of depolarization with carbonyl cyanide *m*-chlorophenyl hydrazone (CCCP) (Figure 1a, Table S1). In some cases, protein turnover was blocked by proteasome inhibition with bortezomib (Btz) or autophagy inhibition with bafilomycin A (BafA) (Table S1). Elevated PARKIN levels were used to increase the likelihood of capturing signal-dependent and mechanistically relevant ubiquitylation events that would otherwise be below the level of detection due to low stoichiometry or abundance.

Using HCT116 cells expressing HA-PARKIN (HCT116[PARKIN], Tier 1), we performed 34 control and QdiGLY experiments (Table S1), quantifying 4772 non-redundant ubiquitylation sites in 1654 proteins (Figure 1a,b). In 18 of these experiments using Btz or CCCP/Btz for 1h, we identified 443 diGLY sites (261 proteins) with log2 Heavy:Light (H:L) ratios 1.0 (2-fold change) in at least one experiment (Figure 1b–c, S2a–c, Table S1,S2), with a Pearson's correlation of 0.69 for two representative experiments (Figure S2e). Sixteen additional Tier 1 experiments with depolarization times up to 10 h identified 537 non-redundant diGLY sites (304 proteins), including 192 diGLY sites (138 proteins) also identified at 1h (Figure S2d). Comparison of log2(H:L) ratios for 48 Tier 1 sites in 36 proteins at 1 and 8 h post CCCP treatment from parallel experiments revealed persistent or increased ubiquitylation for 34 sites when proteasome activity is blocked (Figure S2f).

To systematically determine PARKIN dependence and compare targets in distinct cell lines, we performed 6 QdiGLY experiments in HeLa versus HeLa[PARKIN] cells (Tier 2) with

CCCP/Btz (1h) and reverse SILAC labeling (Figure 1a, Table S1,S2). As expected,[4–7] CCCP-dependent MFN2 poly-ubiquitylation in HeLa cells required PARKIN expression (Figure S2a). We identified 582 PARKIN-dependent diGLY peptides (303 proteins) (Figure 1b), with a Pearson's correlation of 0.88 for duplicate samples (Figure S2e) and significant overlap across biological triplicates (Figure 1d). Importantly, 165 diGLY sites (99 proteins) were common to Tiers 1 and 2 with 1h of depolarization (Figure 1e). This increased to 191 sites (144 proteins) when all Tier1 and Tier 2 data were compared (Table S2). We refer to the overlapping set of ubiquitylation sites with 1h of depolarization and their associated proteins as Class 1 candidate PARKIN-dependent targets while proteins found in both cell lines but with different sites of ubiquitylation are referred to as Class 2 (Table S2). While a 2-fold increase in H:L ratio was used as a threshold for regulated ubiquitylation, many diGLY sites were induced 30–60-fold upon depolarization (Figure 1f, Table S2), indicating highly dynamic target modification via PARKIN.

Class 1 targets were enriched in mitochondrial proteins ($p < 1.76 \times 10^{-17}$), although numerous cytoplasmic proteins were also identified (Figure 2, S2i). In total, 60 Class 1 and 2 targets were linked with mitochondria or ER-type membranes, including 36 MOM proteins. Candidate cytoplasmic targets included proteasome subunits, the VCP/p97 ATPase, and proposed autophagy adaptors (SQSTM1, CALCOCO2/NDP52, and TAX1BP1).

We next performed 22 control and QdiGLY profiling experiments using HCT116 or neuronal SH-SY5Y cells (Tier 3, Figure 1a–b, Table S1, S2), which display primarily mono-ubiquitylated forms of MFN2 ubiquitylation upon depolarization apparently due to low levels of endogenous PARKIN (Figure S2a). Cumulatively, 838 diGLY sites (391 proteins) in HCT116 and 337 diGLY sites (235 proteins) in SH-SY5Y had log2(H:L) 1.0 (Figure 1b), with extensive overlap across Tier 1 and 2 data sets (Figure S2g) and biological triplicates in SH-SY5Y (1h/CCCP) (Figure S2h). Fifteen sites in 12 Class 1 or 2 targets were found in both cell lines, while 29 and 27 CCCP-dependent diGLY sites in 27 and 17 Class 1 or 2 proteins were detected in SH-SY5Y or HCT116 cells, respectively (Figure 2, Table S1, S2). Additionally, 124 Tier 3 sites were identified in 29 Class 1 or 2 proteins that were distinct from Class 1 sites. Thus, many PARKIN-dependent diGLY targets were confirmed at endogenous PARKIN levels. Ubiquitylation of several candidate substrates was demonstrated by immunoblotting, and ubiquitylation was reduced upon PARKIN RNAi for several targets tested (Figure S3a–d).

To complement QdiGLY proteomics, we used anti-HA affinity purification-mass spectrometry (AP-MS),[22] to identify depolarization-dependent high confidence candidate HA-PARKIN-interacting proteins (HCIPs) in duplicate experiments in 293T[PARKIN] cells (Figure 3a, S4a, Table S3), with further validation in HeLa[PARKIN] cells (Figure S4b, Table S4) (see METHODS). Because PARKIN action is dynamic, we examined multiple time points (1, 4, or 8 h) after depolarization in the presence or absence of Btz or BafA. To allow a semi-quantitative assessment of interactions, we compared bait-normalized average assembled peptide spectral matches (APSMs) for proteins that were HCIPs under at least one condition examined unless otherwise noted (Figure 3a, S4a, Tables S3, S4). Without depolarization, no HCIPs were common to both wild-type PARKIN biological duplicates, consistent with PARKIN auto-inhibition prior to activation[23] (Figure 3a, Supplemental

Text). Remarkably, upon depolarization, 4 classes of HCIPs were identified in at least one condition examined (Figure 3a,b): 1) 20 MOM proteins, including MFN1/2, RHOT1/2, and VDACs, HK1/2, the fission protein FIS1 and its interacting protein TBC1D15, and the translocase components TOMM20 and TOMM70, 2) the autophagy adaptors SQSTM1/p62, CALCOCO2 and TAX1BP1, 3) subunits of the catalytic and regulatory particles of the proteasome, and 4) the VCP/p97 ATPase implicated in MFN1 turnover.[7] Nineteen of the 26 mitochondrial and autophagy proteins and 39 of 40 proteasome subunits found in 293T cells were also identified in at least one condition examined in HeLa cells (Figure 3b,S4b). Depolarization-dependent interaction of FLAG-PARKIN with selected endogenous HCIPs was verified by anti-FLAG immunoprecipitation and immunoblotting (Figure S5). Strikingly, 21 of the 27 mitochondrial and autophagy receptor proteins found associated with PARKIN, as well as 8 subunits of the regulatory particle of the proteasome and VCP, were also identified as Class 1 or 2 PARKIN-dependent ubiquitylation targets (Figure 2, 3b, Table S2).

PARKIN activation is thought to reverse auto-inhibition by its N-terminal ubiquitin-like domain (UBL), which has been proposed to sterically hinder E2 interaction with the catalytic center.[20,23] We explored the role of these regions in MOM recruitment, MFN2 ubiquitylation, substrate binding, and proteasome association using 5 mutants (Figure S6a): 1) ΔUBL, lacking the UBL domain (residues 1–80), 2) K27/48R, which blocks ubiquitylation of two regulated diGLY sites in the UBL (Figure 2), 3) S65A and S65E, which block PINK1-dependent phosphorylation of the UBL domain implicated in PARKIN activation *in vitro*,[18] and 4) C431S, removing the active site Cys in RING2. The PD patient mutation PARKIN[C431F] fails to localize to mitochondria in response to depolarization.[15,20] Consistent with this, PARKIN[C431S] failed to localize to mitochondria, efficiently poly-ubiquitylate MFN2, or interact robustly with MOM substrates in response to depolarization (Figure 3a, S6a–d). In contrast, K27/K48R, S65A, and S65E mutants displayed near wild-type activity for localization, MFN2 ubiquitylation, and interaction with MOM proteins at 1 h post depolarization (Figure 3a, S6a–d, Table S3, S6), although we cannot rule out a kinetic effect of these mutations. PARKIN ΔUBL displayed readily detectable association with MOM substrates in the absence of depolarization, consistent with some loss of auto-inhibition,[22] but nevertheless showed enhanced substrate association upon depolarization, suggesting residual PINK1 dependence despite the absence of the UBL and S65. However, MFN2 ubiquitylation was reduced compared with wild-type PARKIN, suggesting reduced ubiquitylation activity. PARKIN ΔUBL also lacked a robust increase in proteasomal binding (Figure 3a).

Our data suggest that PARKIN interacts with and promotes the site-specific ubiquitylation of numerous mitochondrial and cytoplasmic proteins, thereby extending previous studies examining abundance of mitochondrially-enriched proteins.[1,4] To place candidate PARKIN-dependent ubiquitination targets into a structural and functional framework, we have created an interactive resource that integrates dynamic ubiquitylation data with available structural information (Figure S7b–e, and METHODS). We explored the spatial relationship between protein localization, structure, and conservation for 90 Class 1 sites on 36 candidate PARKIN substrates (Figure 4a–d, S7a, Table S5). We found that 90% of ubiquitylated

lysine residues are conserved in mouse, 78% in zebrafish (*D. rerio, Dr*), and 51% in the 29 conserved orthologs in *D. melanogaster* (*Dm*), which harbors an active PARKIN-PINK1 pathway.[6] Moreover, 38% of sites were conserved in all 3 species, and 22 of 36 proteins have at least one site conserved from human to *D. melanogaster* (Figure 4a–d, S7a). DiGLY sites were observed on multiple structural elements (α-helices, β-sheets, and loops) and no obvious sequence motif was identified by MOTIFX, indicating that PARKIN specificity is driven primarily by substrate recruitment and/or proximity rather than specific target sequences.

Of the 17 MOM targets whose structures or membrane orientations are defined, all identified ubiquitylation sites are presented on the cytoplasmic surface (Figure 4c,d), consistent with the idea that PARKIN re-sculpts the MOM proteome via its cytoplasmic recruitment. Fifty-nine percent of Class 1 and 2 targets had one or two sites of ubiquitylation while 41% of targets had 3–15 sites that were PARKIN-dependent based on Tier 2 analysis (Figure S7f). Of the 8 Class 1 and Class 2 sites identified in MFN1, all but 2 are located in helical motifs flanking the 2 C-terminal membrane-spanning regions, suggesting localized ubiquitylation (Figure 2 and Figure 4d). We detected 14 Class 1 and 2 sites in HK1, but unlike MFN1, these sites were comparatively delocalized across both globular domains in HK1 (Figure 4c). Similarly, TOMM70 was decorated extensively over its 10 cytoplasmic TPR motifs (Figure 2,4d). While we cannot exclude the possibility that some ubiquitylation events occur downstream of PARKIN activation, the fact that we find many of the targets as PARKIN-interacting proteins (Figure 3b) is consistent with direct ubiquitylation (see Supplemental Text). An understanding of how PARKIN ubiquitylates topologically diverse proteins and domains within proteins requires further study but will be facilitated by the site-specificity date reported here.

PARKIN appears to promote rapid turnover of some targets but not others. In total, 12 of the Class 1 and 2 proteins identified here (see Figure 2), like MFN1/2 and RHOT1/2,[1,4,7,10,11] likely undergo proteasomal turnover, including C1QBP1 (Figure S3c,d), FIS1, and CISD1, as their total levels are also decreased upon PARKIN activation.[1,4] In contrast, previous studies[4] have identified 50 preferentially cytoplasmic proteins or protein complexes that are enriched in mitochondria in response to depolarization. Consistent with this, we identified 11 of these proteins or components of protein complexes as Class 1 or 2 targets (Figure 2 and S7g), possibly reflecting an under-appreciated dynamic recruitment process impacting mitochondrial homeostasis. These include the autophagy adaptor p62, previously linked with mitochondrial clustering after damage[24], as well as TBC1D15 and DNML1, which are known to interact with FIS1 to regulate fission-fusion cycles.[25] In addition to p62, we also identified candidate autophagy receptors, CALCOCO2 and TAX1BP1, which are ubiquitylated upon depolarization and associate with PARKIN in the presence of BafA (Figure 2,3). Because CALCOCO2 has been shown to target bacteria for autophagy,[26] it is an attractive candidate for involvement in mitophagy. We speculate that these related autophagy adaptor proteins may be dynamically recruited to the MOM and may link the depolarization response to the recruitment of autophagy machinery. Additionally, it is possible that additional cytoplasmic proteins identify here as PARKIN-dependent targets are transiently recruited to mitochondria but below the level of detection in previous studies. It

is also likely that ubiquitylation of PARKIN targets alters their enzymatic properties or functions prior to their turnover by the proteasome or autophagy. Potential PARKIN-regulated functions include: 1) fusion-fission cycles (FIS1, TBC1D15), 2) small molecule transport (VDACs), 3) apoptosis (FKBP8, MCL1, BAX), and 4) iron-sulfur shuttling (CISD1), 5) protein translocation (TOMM70), or 6) proteasome assembly or activity (PSMC subunits) (see Supplemental Text).[25,27]

This work provides systematic target identification and ubiquitylation site-specificity for PARKIN, thereby revealing the diversity and complexity of PARKIN function on the MOM and in the cytoplasm. This resource will enable the development of methods that detect specific diGLY sites in PARKIN targets *in situ*, thus enabling a deeper understanding of how PARKIN controls mitochondrial homeostasis in tissues relevant to Parkinson's Disease.

FULL METHODS

Sample Preparation for diGLY capture

HCT116, HeLa or SH-SY5Y cells (10^8) were grown in lysine free DMEM supplemented with 10% dialyzed FBS (Gibco), 2 mM L-glutamine, pen/strep, and light (K0) lysine (50 μg/mL).[12] Heavy media was the same except the light lysine was replaced with K8-lysine (Cambridge Isotopes) at the same concentration. Where indicated, cells were treated with Btz (1 μM), CCCP (10 μM), and/or BafA (50 nM) for the times indicated. Btz was a gift from Millennium Pharmaceuticals. After the indicated treatments, heavy and light cells were mixed 1:1 by cell number and lysed in 8 mL of denaturing lysis buffer [8 M Urea, 50 mM Tris pH 8.2, 75 mM NaCl, protease inhibitors (EDTA-free, Roche].[12] Samples were incubated on ice for 10 min and then sonicated with $3 \times 10s$ pulses. We typically obtained 30–50mg of total protein. Lysates were digested with trypsin as described previously[28] with one modification. Prior to trypsin digestion, lysates were diluted 1:1 with 50 mM Tris pH 8.2 to lower the urea concentration to 4 M and digested with 10 ng/μl Lys-C (Wako) for 2 hrs at room temperature.

Immunoprecipitation of diGLY containing peptides

Lyophilized peptides from 30–50 mg of digested proteins were resuspended in 1.3 ml of IAP buffer (50 mM MOPS pH 7.4, 10 mM Na_2HPO_4, 50 mM NaCl) and centrifuged at $14,000 \times$ g for 5 minutes to remove any insoluble materials. The supernatant was incubated with α-diGLY antibody coupled to protein A agarose or acrylamide beads for 1hr at 4°C and washed with IAP buffer 3× and once with PBS as described previously.[12] Peptides were eluted by treatment with 50 μl of 5% formic acid for 10 minutes twice. The eluted peptides were desalted using C18 stage-tip method and resuspended in 5% formic acid prior to mass spec analysis. Lysates were subjected to immunoprecipitation sequentially 2 or 4 times, unless otherwise noted in Table S1.

Mass spectrometry analysis of diGLY peptides

Peptides were separated on 100 μm × 20 cm C18 reversed phase (Maccel C18 3μ 200Å, The Nest Group, Inc.) with a 165 min gradient of 6% to 27% acetonitrile in 0.125% formic

acid.[29] The twenty most intense peaks from each full MS scan acquired in the Orbitrap Velos (Thermo) were selected for MS/MS (see RAW files for specific settings).

Sequest-based identification using a Human UNIPROT database followed by a target decoy-based linear discriminant analysis was used for peptide and protein identification as described.[12,30,31] Localization of diGLY sites employed a modified version of the A-score algorithm[32] as described.[12] A-scores > 13 were considered localized. SILAC-based site quantification and signal-to-noise was performed as described previously[12] employing extracted ion chromatograms. The heavy- and light-labeled peptides from each search were subsequently combined using custom scripts. Other parameters used for database searching include: 50 ppm precursor mass tolerance; 1.0 Da product ion mass tolerance; tryptic digestion with up to three missed cleavages; and variable oxidation of Met (+15.994946). For an individual peptide to be used for quantification of sites and proteins, it had to meet one of two conditions: i) Both heavy and light isotopic envelopes must be detected with signal-to-noise ratios above 5.0; ii) One isotopic envelope (heavy or light) must have a signal-to-noise ratio above 10.0. Equal mixing ratios for heavy to light cells were confirmed by calculating the mean log2(H:L) ratios in non-diGLY non-lysine containing peptides and subtracting that from the corresponding log2(H:L) diGLY ratios if necessary. Keratins were removed from site lists. Contributions of peptide identifications to various protein isoforms were condensed into a single UNIPROT descriptor using principles of parsimony. Mass spectrometry RAW files are available upon request.

Interaction Proteomics

Interaction proteomics was performed essentially as described previously, but with small modifications.[22] Briefly, 293T or HeLa cells were transduced with a lentiviral vector expressing HA-FLAG-PARKIN (NP_004553.2) or the designated PARKIN mutants, and stable cell lines selected in puromycin. Cells from 4×15 cm dishes at 80% confluence were treated with CCCP (10 μM), Btz (1 μM), and/or BafA (50 nM) as indicated and after the indicated time, cells were harvested and lysed in 3 ml of 50 mM Tris-HCl [pH 7.4], 150 mM NaCl, 0.5% Nonidet P40, and protease inhibitors. Cleared lysates were filtered through 0.45 μm spin filters (Millipore Ultrafree-CL) and immunoprecipitated with 30 μl anti-HA resin (Sigma). Complexes were washed 4× with lysis buffer, exchanged into PBS for a further 3 washes, eluted with HA peptide, reductively carboxymethylated, and precipitated with 10% TCA. TCA-precipitated proteins were trypsinized, purified with Empore C18 extraction media (3 M), and analyzed via LC-MS/MS with a LTQ-Velos linear ion trap mass spectrometer (Thermo) with an 18 cm^3 125 μm (ID) C18 column and a 50 min 8%–26% acetonitrile gradient. All AP-MS experiments in 293T cells were performed in biological duplicates and for each biological experiment, complexes were analyzed twice by LC-MS to generate technical duplicates. AP-MS experiments in HeLa cells were performed on a single IP but with technical duplicates. Spectra were searched with Sequest against a target-decoy human tryptic UNIPROT-based peptide database, and these results were loaded into the Comparative Proteomics Analysis Software Suite (*CompPASS*) to identify high confidence candidate interacting proteins (HCIPs).[22] Here, a stats table derived from analogous AP-MS data for 166 unrelated proteins was employed to determine weighted and normalized D-scores (WD^N-score) as well as Z-scores based on spectral counts. The D-score measures the

reproducibility, abundance, and frequency of individual proteins detected in each individual analysis.

To identify PARKIN associated proteins, we filtered proteins at a 2% false discovery rate for those with a WD^N-score 1.0, Z-score 5, and average assembled peptide spectral matches (APSMs) 2 in both biological duplicates. In addition to the initially identified proteins, APSMs for interactors with WD^N-scores greater than 1 under at least one condition examined, or with a Z-score greater than 10 in both biological duplicates, were plotted in heatmap form using Multi-experiment Viewer (MeV). Due to space limitations, a subset of proteins which had a WD^N-score 1.0 in at least one experiment were omitted from Figure 3 but are contained in the heat maps in Figure S4 as well as Tables S3 and S4. TAX1BP1 that was identified in PARKIN immunoprecipitates and also found to be ubiquitylated but did not pass the stringent cut-off for passing our scoring scheme was also displayed in the heat map. We note that while several proteins passed the WD^N-score cut-off for PARKIN associated proteins in the absence of depolarization in individual experiments, there was essentially no overlap within biological duplicates (Table S4). In addition, for proteins with a maximum of 1–3 spectral counts, it is possible that those proteins were missed under some conditions due to stochastic sampling of low abundance proteins by LC-MS (e.g. CYB5R3, TOM22, and RHOT1 with wild-type PARKIN at 8 h post CCCP in the presence versus the absence of BafA, Figure 3a). The following proteins were identified in only 1 biological duplicate as being associated with PARKIN but were included in the heatmap (Figure 3a) as they are also present as Class 1 diGLY targets: SQSTM1, TAX1BP1, TBC1D15, MYO6, VCP, RHOT2, HK2, MDH2, CYB5R3, and ACSL4.

Immunological Methods and Microscopy

To validate interactions between PARKIN and candidate interacting proteins (Figure S3), 293T cells stably expressing HA-FLAG-PARKIN were either left untreated or treated with CCCP (10 μM) or CCCP (10 μM) and Btz (1 μM) for 1 h. Extracts [50 mM Tris-HCl [pH 7.4], 150 mM NaCl, 0.5% Nonidet P40, and protease inhibitors] from cells were subjected to immunoprecipitation with anti-FLAG resin (M2 agarose; Sigma), and washed complexes subjected to immunoblotting with the indicated antibodies. To examine MFN2 ubiquitylation, extracts from cells lysed in denaturing lysis buffer [8 M urea, 75 mM NaCl, 50 mM Tris, [pH 8.0], and protease inhibitors] expressing the indicated HA-FLAG-PARKIN mutant proteins were separated on a 4–12% gradient SDS-polyacrylamide gel (PAGE) and blotted with anti-HA or anti-MFN2. To examine PARKIN levels in the cell lines employed (Figure S1), cells were lysed in denaturing lysis buffer and protease inhibitors and extracts subjected to SDS-PAGE and immunoblotting. To examine ubiquitylation of candidate PARKIN substrates by immunoblotting, HCT116 cell lines stably expressing the candidate substrates C-terminally tagged with HA-FLAG epitopes were transfected with either control siRNA or an siRNA targeting *PARKIN* (#1: 5'-GGAGUGCAGUGCCGUAUUU-3', #2: 5'-GUAAAGAAGCGUACCAUGA-3', #3: 5'-GGAGCCAUCGCCUAUGAAA-3', #4:5'-GUAAAGAAGCGUACCAUGA-3', Thermo Scientific). After 72 h, cells were treated with CCCP (10 μM) ± the presence of Btz to block proteasomal turnover of targets. At the indicated times, cells were lysed in 8 M urea and subjected to immunoblotting using anti-HA antibodies. Identical gels were run and probed

with anti-PCNA as a loading control. The antibodies used are as follows: anti-TOMM70, (Proteintech, 14528-1); anti-MFN2, (Epitomics, 3272-1 or Sigma, WH0009927M3); anti-ADRM1, (Enzo Scientific, BML-PW9910); anti-Rpn10, (Enzo Scientific, BML-PW9250); anti-HK1, (Cell Signaling, C35C4); anti-PSMD2, (Affinity BioReagents, PA1-964); anti-PARKIN, (PRK8, Santa Cruz, sc-32282).

To examine the localization of PARKIN and various PARKIN mutants, HeLa cells stably expressing HA-FLAG-tagged proteins were plated on No.1 coverslips, treated with CCCP (10 μM, 1h), and fixed with 4% paraformaldehyde prior to immunofluorescence using anti-HA to detect PARKIN proteins and anti-TOMM20 to detect mitochondria. All images were collected with a Yokogawa CSU-X1 spinning disk confocal on a Nikon Ti-E inverted microscope equipped with 100× Plan Apo NA 1.4 objective lens. HA-PARKIN fluorescence was excited with the 491nm line (selected with an AOTF) from Spectral Applied Precision LMM-7 solid state laser launch. Emission was collected with a quad band pass polychroic mirror (Semrock) and a Chroma ET525/50m emissions filter. TOMM20 fluorescence was excited with the 561nm line from the LMM-7 launch, and emission collected with the Semrock polychroic and a Chroma ET620/60m emission filter. Images were acquired with a Hamamatsu ORCA-AG cooled CCD camera controlled with MetaMorph 7 software. Nine z-series optical sections were collected with a step size of 0.2 microns, using the internal Nikon Ti-E focus motor. Z-series were deconvolved using AutoQuant blind deconvolution software, and are displayed as maximum z-projections. Gamma and brightness were adjusted on displayed images (identically for compared image sets) and percent colocalization was calculated by thresholding for signal at least 4 standard deviations above background in a single z slice (identically for compared image sets) using MetaMorph 7 software (Table S6).

Structural Analysis of Ubiquitylation Sites and Web Portal

Using the Uniprot identifier for each protein identified, the corresponding PDB file(s) (if available) were determined using data from the UniProt to PDB cross-reference table (http://www.ebi.ac.uk/pdbe/docs/sifts/quick.html). The amino acid position in the structure corresponding to each ubiquitylation site was calculated based on their relative position in the structure using the information provided by the cross reference table. Data for each experiment was stored in MySQL tables, which are used when accessing the data via the web portal. For rendering of the structural information via the web portal, Jmol: an open-source Java viewer for chemical structures in 3D (http://www.jmol.org/) was used. Access to the web portal is available at: harper.hms.harvard.edu.

Gene Ontology

Gene ontology analysis was performed using DAVID.[33] Additional sub-cellular localization parameters as designated in Figure 2 were performed manually using MITOCARTA, Human Protein Atlas, and Genbank.

Supplementary Material

Refer to Web version on PubMed Central for supplementary material.

Acknowledgments

References

1. Narendra DP, Walker JE, Youle R. Mitochondrial Quality Control Mediated by PINK1 and Parkin: Links to Parkinsonism. Cold Spring Harb Perspect Biol. 2012; 4:a011338. [PubMed: 23125018]

2. Youle RJ, Narendra DP. Mechanisms of mitophagy. Nat Rev Mol Cell Biol. 2011; 12:9–14. [PubMed: 21179058]

3. Dawson TM, Dawson VL. The role of parkin in familial and sporadic Parkinson's disease. Mov Disord. 2010; 25(Suppl 1):S32–S39. [PubMed: 20187240]

4. Chan NC, et al. Broad activation of the ubiquitin-proteasome system by Parkin is critical for mitophagy. Hum Mol Genet. 2011; 20:1726–1737. [PubMed: 21296869]

5. Glauser L, Sonnay S, Stafa K, Moore DJ. Parkin promotes the ubiquitination and degradation of the mitochondrial fusion factor mitofusin 1. J Neurochem. 2011; 118:636–645. [PubMed: 21615408]

6. Ziviani E, Tao RN, Whitworth AJ. Drosophila parkin requires PINK1 for mitochondrial translocation and ubiquitinates mitofusin. Proc Natl Acad Sci U S A. 2010; 107:5018–5023. [PubMed: 20194754]

7. Tanaka A, et al. Proteasome and p97 mediate mitophagy and degradation of mitofusins induced by Parkin. J Cell Biol. 2010; 191:1367–1380. [PubMed: 21173115]

8. Poole AC, Thomas RE, Yu S, Vincow ES, Pallanck L. The mitochondrial fusion-promoting factor mitofusin is a substrate of the PINK1/parkin pathway. PLoS ONE. 2010; 5:e10054. [PubMed: 20383334]

9. Sun Y, Vashisht AA, Tchieu J, Wohlschlegel JA, Dreier L. VDACs recruit Parkin to defective mitochondria to promote mitochondrial autophagy. J Biol Chem. 2012; 287:40652–40660. [PubMed: 23060438]

10. Wang X, et al. PINK1 and Parkin target Miro for phosphorylation and degradation to arrest mitochondrial motility. Cell. 2011; 147:893–906. [PubMed: 22078885]

11. Liu S, et al. Parkinson's disease-associated kinase PINK1 regulates Miro protein level and axonal transport of mitochondria. PLoS Genet. 2012; 8:e1002537. [PubMed: 22396657]

12. Kim W, et al. Systematic and quantitative assessment of the ubiquitin-modified proteome. Mol Cell. 2011; 44:325–340. [PubMed: 21906983]

13. Wagner SA, et al. A proteome-wide, quantitative survey of in vivo ubiquitylation sites reveals widespread regulatory roles. Mol Cell Proteomics. 2011; 10 M111 013284.

14. Wenzel DM, Lissounov A, Brzovic PS, Klevit RE. UbcH7-reactivity profile reveals Parkin and HHARI to be RING/HECT hybrids. Nature. 2011; 474:105–108. [PubMed: 21532592]

15. Joselin AP, et al. ROS-dependent regulation of Parkin and DJ-1 localization during oxidative stress in neurons. Hum Mol Genet. 2012; 21:4888–4903. [PubMed: 22872702]

16. Narendra D, Tanaka A, Suen DF, Youle RJ. Parkin is recruited selectively to impaired mitochondria and promotes their autophagy. J Cell Biol. 2008; 183:795–803. [PubMed: 19029340]

17. Lazarou M, Jin SM, Kane LA, Youle RJ. Role of PINK1 binding to the TOM complex and alternate intracellular membranes in recruitment and activation of the E3 ligase Parkin. Dev Cell. 2012; 22:320–333. [PubMed: 22280891]

18. Kondapalli C, et al. PINK1 is activated by mitochondrial membrane potential depolarization and stimulates Parkin E3 ligase activity by phosphorylating Serine 65. Open Biol. 2012; 2:120080. [PubMed: 22724072]

19. Sha D, Chin LS, Li L. Phosphorylation of parkin by Parkinson disease-linked kinase PINK1 activates parkin E3 ligase function and NF-kappaB signaling. Hum Mol Genet. 2010; 19:352–363. [PubMed: 19880420]

20. Lazarou M, Narendra DP, Jin SM, Tekle E, Banerjee S, Youle RJ. PINK1 drives Parkin self-association and HECT-like E3 activity upstream of mitochondrial binding. J Cell Biol. 2013; 200:163–172. [PubMed: 23319602]

21. Geisler S, et al. PINK1/Parkin-mediated mitophagy is dependent on VDAC1 and p62/SQSTM1. Nat Cell Biol. 2010; 12:119–131. [PubMed: 20098416]

22. Sowa ME, Bennett EJ, Gygi SP, Harper JW. Defining the human deubiquitinating enzyme interaction landscape. Cell. 2009; 138:389–403. [PubMed: 19615732]

23. Chaugule VK, et al. Autoregulation of Parkin activity through its ubiquitin-like domain. Embo J. 2011; 30:2853–2867. [PubMed: 21694720]

24. Narendra D, Kane LA, Hauser DN, Fearnley IM, Youle RJ. p62/SQSTM1 is required for Parkin-induced mitochondrial clustering but not mitophagy; VDAC1 is dispensable for both. Autophagy. 2010; 6:1090–1106. [PubMed: 20890124]

25. Onoue K, et al. Fis1 acts as mitochondrial recruitment factor for TBC1D15 that is involved in regulation of mitochondrial morphology. J Cell Sci. in press.

26. von Muhlinen N, et al. LC3C, Bound Selectively by a Noncanonical LIR Motif in NDP52, Is Required for Antibacterial Autophagy. Mol Cell. 2012; 48:29–42.

27. Huang P, Galloway CA, Yoon Y. Control of mitochondrial morphology through differential interactions of mitochondrial fusion and fission proteins. PLoS ONE. 2011; 6:e20655. [PubMed: 21647385]

28. Villen J, Gygi SP. The SCX/IMAC enrichment approach for global phosphorylation analysis by mass spectrometry. Nat Protoc. 2008; 3:1630–1638. [PubMed: 18833199]

29. Haas W, et al. Optimization and use of peptide mass measurement accuracy in shotgun proteomics. Mol Cell Proteomics. 2006; 5:1326–1337. [PubMed: 16635985]

30. Huttlin EL, et al. A tissue-specific atlas of mouse protein phosphorylation and expression. Cell. 2010; 143:1174–1189. [PubMed: 21183079]

31. Eng JK, McCormack AL, Yates JR 3rd. An approach to correlate tandem mass spectral data of peptides with amino acid sequences in a protein database. J Am Soc Mass Spectrom. 1994; 5:976–989. [PubMed: 24226387]

32. Beausoleil SA, Villen J, Gerber SA, Rush J, Gygi SP. A probability-based approach for high-throughput protein phosphorylation analysis and site localization. Nat Biotechnol. 2006; 24:1285–1292. [PubMed: 16964243]

33. Huang da W, Sherman BT, Lempicki RA. Systematic and integrative analysis of large gene lists using DAVID bioinformatics resources. Nat Protoc. 2009; 4:44–57. [PubMed: 19131956]
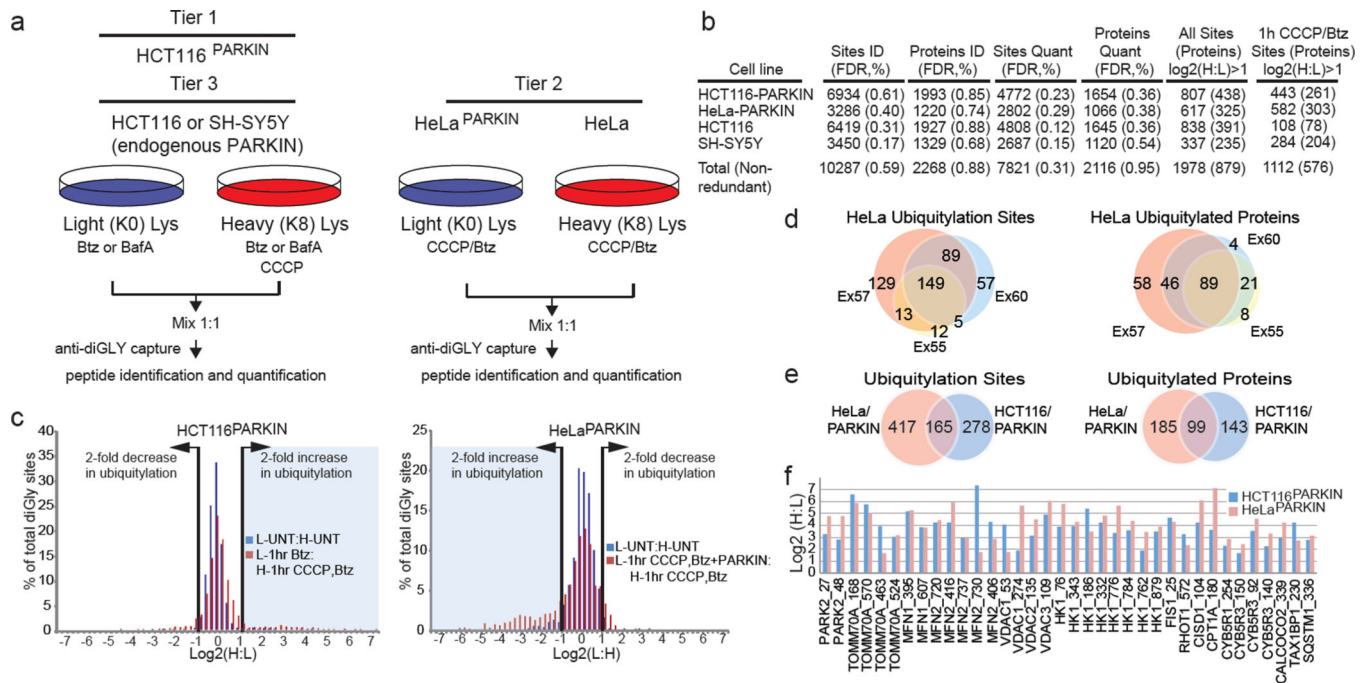
Figure 1. QdiGLY proteomics for PARKIN-dependent ubiquitylation

a, Proteomics work flow. **b**, diGLY sites identified and quantified across 73 experiments. FDR, false discovery rate. **c**, log2(H:L) plots for quantified diGLY peptides for HCT116[PARKIN] (experiment 17) or HeLa[PARKIN] (experiment 57) cells (Table S2). **d**, Overlap of ubiquitylation sites in HeLa[PARKIN] biological triplicates (1h CCCP + Btz) (Table S1, S2). **e**, Ubiquitylation site and protein overlap between all HCT116[PARKIN] and HeLa[PARKIN] experiments treated with CCCP and Btz for 1h. **f**, log2(H:L) ratios for selected diGLY sites from HCT116[PARKIN] (Ex 17) and HeLa[PARKIN] (Ex 57) (1h CCCP + Btz).
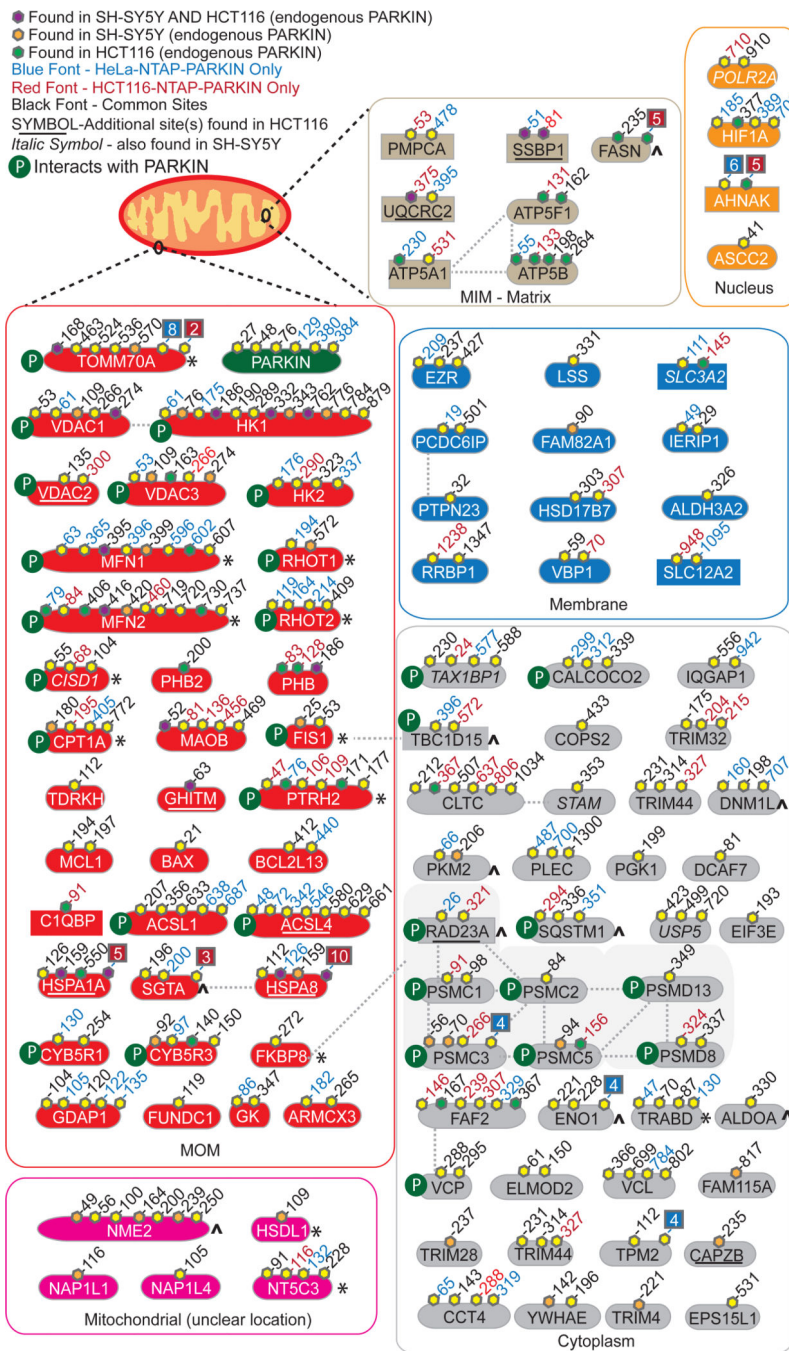
Figure 2. PARKIN-dependent ubiquitylation sites revealed by QdiGLY proteomics

Class 1 sites are in black font. Additional sites found in Class 1 proteins are in red (HCT116[PARKIN]) or blue font (HeLa[PARKIN]). Site overlap in HCT116 and/or SH-SY5Y: magenta, orange, and green octagons. Dotted lines: interacting proteins. Rectangles represent Class 2 substrates. Red or blue boxes refer to additional sites identified in either HCT116[PARKIN] and HeLa[PARKIN] cells (Table S2). * and ^, protein levels decrease or increase, respectively, upon depolarization.[4]
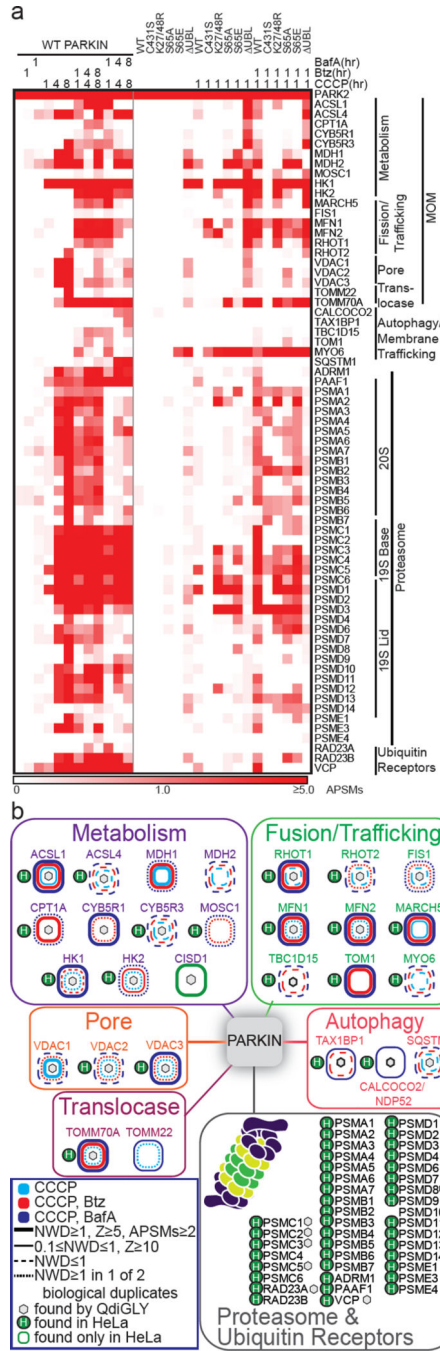
Figure 3. PARKIN associates with mitochondrial proteins and the proteasome in response to depolarization

a, Heat map of HCIPs (represented by APSMs) for HA-FLAG-PARKIN and mutants in response to depolarization in 293T cells, with or without Btz or BafA. Proteins indicated had WD^N-scores 1.0, Z-score 5, and APSMs 2 unless otherwise noted (see METHODS).**b**, Summary of PARKIN-interacting proteins in 293T and HeLa and integration with diGLY sites.
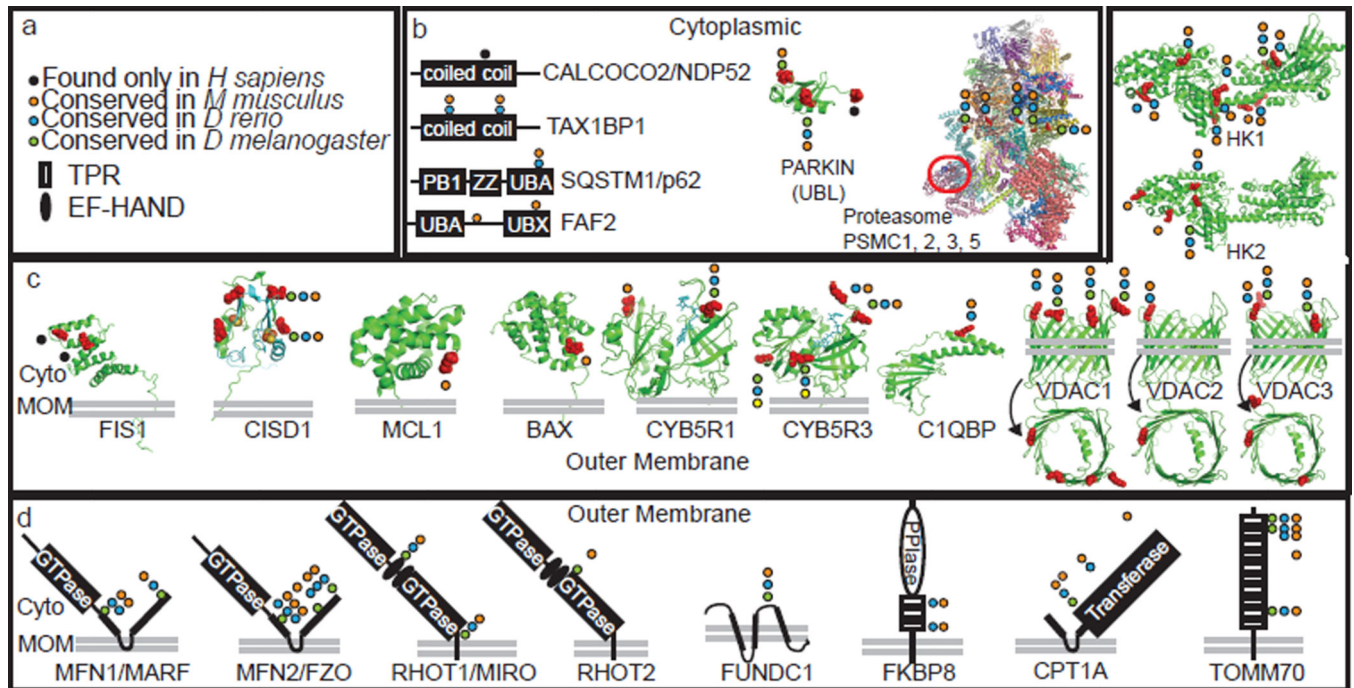
Figure 4. Structural anatomy and conservation of PARKIN-dependent diGLY sites
Structures or domain schematics are shown for Class 1 depolarization and PARKIN-dependent diGLY sites (PDB codes, Table S5). Color-coded circles (**a**) indicate the conservation of Lys at the homologous position in *M. musculus, D. rerio*, and *D. melanogaster* (Table S5). For structures, regulated sites are shown in red space-filled models. **b**, Cytoplasmic proteins. RPN10, red circle. **c**, MOM proteins with structures. **d**, MOM proteins without structures.